2026 IEEE International Conference on Robotics and Automation (ICRA 2026)
June 1-5, 2026. Vienna, Austria

Multi-Robot Informative Sampling and Coverage in GPS-Denied Environments

Aiman Munir Ehsan Latif Ramviyas Parasuraman

***Abstract*— Multi-Robot Systems (MRS) in GPS-denied environments such as indoor spaces, subterranean areas, and urban canyons face the dual challenge of localizing themselves while performing informative path planning (IPP) to model unknown spatial fields. Current IPP methods rely heavily on GPS for localization, limiting their applicability in GPS-denied settings, while existing approaches addressing observation uncertainty fail to account for the localization uncertainty that degrades mapping accuracy. This paper presents Anchor-Oriented IPP (AO-IPP), a framework that coordinates robot teams through relative positioning using Access Points and uncertainty-driven transitions between three phases: anchor point localization, informative sampling for field estimation, and spatial coverage optimization. Each robot maintains dual Gaussian Process models with transitions driven by uncertainty levels rather than fixed time schedules. Extensive simulations and real-world experiments demonstrate that AO-IPP achieves performance comparable to GPS-based IPP algorithms while outperforming existing methods in balancing IPP and coverage objectives by up to 54%. The approach exhibits sublinear regret bounds and enables autonomous coordination in challenging environments previously inaccessible to traditional IPP methods, providing a robust solution for environmental monitoring, exploration, and mapping applications requiring both accurate field estimation and comprehensive spatial coverage.**

I. Introduction

Informative Path Planning (IPP) enables autonomous robots to strategically survey areas and model unknown spatial fields through data-driven sampling of environmental phenomena such as temperature distributions or radio signals [1]. This approach has proven essential across diverse applications including environmental monitoring [2], search and rescue operations [3], and precision agriculture [4], where the primary objective involves maximizing information gain while optimizing resource constraints such as mission time and energy [5].

Traditional IPP methods employ Gaussian Processes (GPs) with Bayesian sampling techniques to reconstruct underlying spatial fields and maximize information gain [6]. However, these approaches fundamentally depend on GPS availability for robot localization within global reference frames [7], [8]. While effective in open environments with strong GPS signals [9], [10], this dependency severely limits applicability in GPS-denied settings including indoor environments, subterranean spaces, and urban canyons [11]. Critically, observation uncertainty in GP-based field inference differs from localization uncertainty, with the latter potentially biasing sampling decisions and degrading mapping accuracy. Although active SLAM approaches [12] and uncertainty-aware exploration methods [13], [14] address pose uncertainty, they typically assume consistent global frames through SLAM back-ends or drift-bounded odometry.

School of Computing, University of Georgia, USA. Emails: {aiman.munir, ehsan.latif, ramviyas}@uga.edu

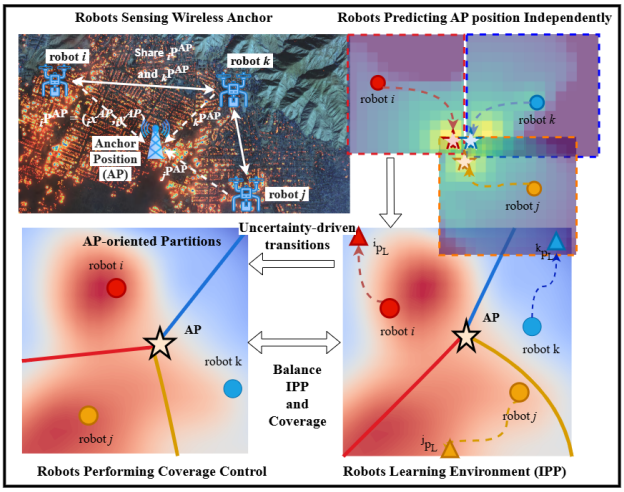

Fig. 1. Overview of the proposed AO-IPP, which balances the objectives of the AP localization, spatial field estimation (IPP), and spatial coverage using a novel uncertainty-driven transition strategy.

Recent advances have incorporated observation uncertainty into IPP frameworks [15], [16], enabling adaptive path planning based on data confidence levels. However, significant gaps remain in developing IPP strategies for completely GPS-denied environments. Furthermore, while recent works explore balancing IPP with spatial coverage objectives [17], [16], they rely on fixed time-bounded transitions rather than adaptive uncertainty-driven strategies, limiting their effectiveness in dynamic environments [18].

This work addresses these limitations by proposing AO-IPP, a framework specifically designed for MRS operating in GPS-denied environments. Our approach leverages relative position measurements from identifiable anchor points such as cell towers or WiFi routers, integrating localization uncertainty directly into the IPP process. The framework assumes robots can obtain noisy relative measurements from the anchor points while lacking global positioning access. The mission requires simultaneous accomplishment of three objectives: localizing relative to anchor points, learning spatial field distributions through strategic sampling, and achieving effective coverage for comprehensive monitoring.

Our control strategy balances localization improvement with informative exploration through uncertainty-driven phase transitions, enabling efficient environmental mapping without global coordinates. See Fig. 1 for a depiction of the proposed AO-IPP framework, which extends IPP applications to complex domains including subterranean exploration and extraterrestrial surface mapping [19], while providing robust multi-robot coordination capabilities in challenging

environments [16], [20].

The key contributions of this work include:

- The introduction of a novel framework that explicitly integrates localization and information uncertainty within multi-robot active sampling and IPP processes, employing a control algorithm that enables seamless transitions between localization improvement, information-driven exploration, and coverage control based on uncertainty levels in anchor point and field estimations.
- We provide a theoretical analysis of regret bounds demonstrating near-optimal performance in localization and coverage tasks, supported by extensive experimental validation using simulations and real-world datasets that confirm the approach's capability and scalability for GPS-free exploration in challenging environments.

II. Related Work

The exploration of Informative Path Planning (IPP) in robotic systems has garnered substantial interest, aiming to optimize autonomous exploration and data acquisition in various environments. Recent studies integrated sophisticated modeling techniques and distributed decision-making processes for IPP. [19] introduced an innovative approach that employs regression with Sparse Gaussian Processes (GPs), utilizing the capabilities of GPs to make informed decisions based on sparse observations efficiently. Similarly, Jang et al. [21] explored fully distributed informative planning, presenting a framework that allows multi-robot systems to learn about environmental phenomena. Their work emphasizes the potential of distributed approaches in enhancing the autonomy and adaptability of robotic systems, particularly in dynamic or uncertain environments.

Most IPP research assumes GPS availability, enabling precise localization and navigation. For example, [22] introduced an IPP for radiological surveys, balancing exploration-exploitation in non-convex scenarios, while [23] used intent-based deep reinforcement learning for multi-agent IPP in GPS-guided environments. Studies like [24], [25] explored adaptive sampling and distributed modeling in GPS-assumed contexts, demonstrating the potential of heterogeneous MRS in environmental monitoring. In [7], a distributed approach balanced informative sampling and connectivity under communication constraints. While these studies advance GPS-based IPP, they also highlight challenges in GPS-denied environments. Schmid et al. [15] proposed a sampling-based approach for online IPP in uncharted environments, with real-time path adaptation. Works by [26] and [27] expanded IPP to multi-robot coordination for covering unknown fields, but still rely on external positional data.

Recent research begins to address localization uncertainty in IPP strategies. Min et al. [20] focused on target localization in GPS-denied environments, assuming precise initial robot positions but addressing control imperfections. Another study [3] tackled localization uncertainty in single-robot IPP with high computational demands, assuming a localization algorithm within a global frame. In contrast, our research uniquely incorporates localization uncertainty into multi-robot IPP in GPS-denied settings, leveraging multi-robot coordination under limited resources. Recent work [17] and [16] argues for a balancing controller that shifts its strategy from an IPP objective to a coverage objective, assuming the IPP process gets completed within a fixed mission duration. However, large-scale applications require adaptive transitions to lower uncertainties, which generally informs the completion of the IPP objective.

Our proposed anchor-oriented multi-robot IPP and coverage approach aims to overcome the limitations highlighted in the literature. Leveraging only the relative position measurements and dynamic Voronoi partitioning around an anchor point (AP) to determine workable bounds for optimal IPP enhances the applicability of IPP to a wider range of environments. We introduce a robust framework for distributed decision-making and environmental exploration without reliance on external positional references. In [28], the authors developed an anchor-oriented coverage controller that enables relative localization of robots using a common Access Point (AP). But, it did not address the IPP objectives nor the problem of balancing the IPP and coverage objectives, which require careful devising of Bayesian sampling aided by the uncertainties in the process. In contrast, our algorithm employs a similar anchor-oriented approach for IPP, dynamically transitioning from localization to learning to coverage, which facilitates the reconstruction of the underlying spatial distribution in challenging GPS-denied environments, and optimizes multiple objectives seamlessly.

III. Anchor-Oriented Informative Path Planning and Spatial Coverage

In this section, we will first formulate the GPS-denied IPP problem and then describe the proposed distributed controller for multi-robot IPP along with its theoretical properties.

A. Problem Formulation

In distributed multi-robot systems operating within environments devoid of global positioning frameworks, a pivotal challenge arises in executing cooperative tasks without access to a unified coordinate system. Such a scenario is quintessential in environments where GPS is unreliable or non-existent, demanding a strategy for robots to collaboratively cover an area or gather environmental data. This problem can be formulated as: *Develop a distributed control approach for multi-robot IPP capable of estimating the underlying spatial distribution without global positioning.* We consider a scenario wherein each robot can detect an AP and estimate its location with a certain degree of uncertainty, modeled as a Gaussian distribution $N(\mu^{\mathrm{AP}}, \sigma^{2^{\mathrm{AP}}})$ The estimation of the AP's location is refined through Bayesian inference, utilizing onboard sensory inputs and local odometry data from an Inertial Measurement Unit (IMU). The inference of the Anchor Point (AP) position enables the robot to localize other robots solely based on the relative positions of the AP and the positions of other robots within their local Frame of Reference (FoR).The local position estimation then enables robots to learn spatial information of

the target workable environment collaboratively. To perform IPP, robots must have optimal coverage of the environment, for which we use anchor-oriented spatial coverage.

B. Anchor-Oriented Spatial Coverage

Coverage control optimizes the spatial distribution of the robot to maximize the effectiveness of area monitoring, while IPP strategically selects sampling locations to maximize information gain on spatial phenomena. Traditional IPP implicitly assumes coverage through exploration, whereas our approach explicitly manages the transition from information gathering to spatial optimization as field knowledge becomes sufficient. This transition is critical in resource-constrained missions where robots must balance exploration with coverage requirements. A common method for this involves partitioning the environment into regions using Voronoi partitions. For n robots in $R = \{1, 2, \ldots, n\}$ tasked with inferring a spatial distribution in a region $\mathcal{D} \subset \mathbb{R}^2$, let $\mathbf{p}_i \in \mathcal{D}$ denote the position of robot i, and q be any point within the workspace $\mathcal{D}$. The Voronoi partition $\mathcal{V}_i$ for each robot $i \in R$ is defined as:

$$\mathcal{V}_i = \{q \in \mathcal{D} \mid \|q - \mathbf{p}_i\| \leq \|q - \mathbf{p}_j\|, \forall j \neq i\}. \quad (1)$$

Here, $\|\cdot\|$ denotes the Euclidean norm. Coverage quality is quantified through the locational cost, defined as:

$$H_V(\mathbf{p}_1, ..., \mathbf{p}_n) = \sum_{i=1}^{n} \int_{\mathcal{V}_i} \frac{1}{2} \|q - \mathbf{p}_i\|^2 \phi(q) dq, \quad (2)$$

where $\phi(q) : \mathcal{D} \to \mathbb{R}_{>0}$ describes the importance of a given point q [29]. The objective is to minimize this locational cost to achieve optimal coverage. A necessary condition for optimal coverage is that each robot should be positioned at the centroid of its respective region [1], calculated as:

$$\mathbf{C}_i = \frac{\int_{\mathcal{V}_i} q\phi(q)\, dq}{\int_{\mathcal{V}_i} \phi(q)\, dq}, \quad (3)$$

This condition is typically achieved by following the negative gradient descent of the locational cost using Lloyd's algorithm [30], expressed as:

$$\dot{p}_i = \kappa(\mathbf{C}_i - \mathbf{p}_i), \quad \kappa > 0, \quad (4)$$

which results in a Centroidal Voronoi Tessellation (CVT). However, CVTs are not unique, and thus this approach only guarantees convergence to a local minimum of the locational cost in Eq. (2).

In a GPS-denied setting, robots lack prior knowledge of the positions of other robots in a global FoR. As a result, each robot i navigates using its local FoR, while estimating the positions of other robots relative to its own FoR. To address this challenge, we adapt the Voronoi partitioning approach for this specific context. The position of robot j in robot i's FoR is denoted by $\mathbf{p}_{(i,j)}$, and the robot's own position by $\mathbf{p}_i$. Each robot is aware of the boundary size, $\mathcal{D}_i \subset \mathbb{R}^2$, centered around an anchor point $\mathbf{p}_i^{\text{AP}}$ with a radius r. This local environment is defined as:

$$\begin{aligned}\mathcal{D}_i = \{q_i = (x_i^q, y_i^q) \mid \big\|(x_i{}^q - x_i^{\text{AP}}) + (y_i^q - y_i^{\text{AP}})\big\| \\ + \big\|(x_i^q - x_i^{\text{AP}}) - (y_i^q - y_i^{\text{AP}})\big\| \leq 2r\},\end{aligned} \quad (5)$$

Assuming a common anchor point, we infer:

$$\mathbf{p}_{(i,j)} - \mathbf{p}_i^{\text{AP}} = \mathcal{R}_{(i,j)}(\mathbf{p}_j - \mathbf{p}_j^{\text{AP}}), \quad (6)$$

where $\mathcal{R}_{(i,j)}$ is a rotation matrix transforming coordinates from j to i. The AP-oriented partitioning $\mathbf{V}_i$ is defined as:

$$\begin{aligned}\mathbf{V}_i\left(\mathbf{p}_{(i,j)}\right) = \{q_i \in \mathcal{D}_i \mid \big\|(q_i - \mathbf{p}_i^{\text{AP}}) - (\mathbf{p}_i - \mathbf{p}_i^{\text{AP}})\big\| \leq \\ \big\|(q_i - \mathbf{p}_i^{\text{AP}}) - \mathcal{R}_{(i,j)}(\mathbf{p}_j - \mathbf{p}_j^{\text{AP}})\big\|, \forall j \in \mathbb{R}\}.\end{aligned} \quad (7)$$

In this context, each robot independently applies its coverage control law using Eq. 4, guided by the adapted anchor-oriented Voronoi partitioning described in Eq. 7.

Coverage control literature typically assumes that the density function is known [31]. However, this assumption is not practical in real-world scenarios. In our approach, we address this by learning the density function using informative sampling before proceeding with the coverage task similar to [32], [17], [16].

C. Anchor-Oriented IPP (AO-IPP)

Multi-robot IPP aims to plan trajectories for n robots that collectively enable accurate estimation of a spatial phenomenon. Each robot, operating within its Voronoi partition, selects goal points iteratively based on the information gain. The information gain $I(q)$ of each point q in the workspace:

$$I(q) = \alpha \times \mu(q) + \beta \times \sigma^2(q), \quad \text{where} \quad \alpha + \beta = 1. \quad (8)$$

Here, α and β denote the weight values for mean $\mu(q)$ and variance $\sigma^2(q)$ of the region at point q estimated using a model such as Gaussian Process Regression (GPR).

1) GPR for IPP: GPR is a non-parametric method that captures an unknown function's characteristics by defining a prior distribution over the function space. The observations of the distribution function $\phi(q)$ at any point q are modeled as $y = f(q) + \epsilon$, where ϵ is Gaussian noise. A GP is defined by its mean function $u(q)$ and covariance function $k(q, q')$, where q' is the test location. The GP can be represented as:

$$\phi(q) \sim \mathcal{GP}(\mu(q), k(q, q')),$$

GP upper confidence bound (GP-UCB) is among the popular choices for determining the information gain among points [5], [7]. Using GP-UCB, we predict f^* for unobserved points $Q^* = \{q_1^*, q_2^*, \ldots, q_m^*\} \in \mathcal{D} \setminus Q$. The posterior mean and variance of $f(q^*)$ at a test location q^* are given by:

$$\begin{aligned}\mu[f^*] &= \mu(q*) + k^\top(\mathcal{K} + \sigma_n^2 I)^{-1}(y - \mu(q*)), \\ \sigma^2[f^*] &= k^* - k^\top(\mathcal{K} + \sigma_n^2 I)^{-1}k,\end{aligned} \quad (9)$$

where $\mathcal{K}$ is the covariance matrix between the training points, k is the covariance between training and test points, and k^* is the covariance between test points.

2) Dual IPP: In this study, we utilize two mutually exclusive GPR models for each robot: one for predicting the AP location (modeled as Wi-Fi signals) and another for mapping the spatial phenomenon (modeled as a multivariate Gaussian process representing the physical distribution $\phi(\cdot)$). These are referred to as the AP distribution and Field distribution, respectively. Each robot maintains its estimates of AP and robots' locations in its local FoR and only shares field distribution training data to enhance predictions.

D. Proposed Balancing controller

The proposed AO-IPP controller enables each robot to adaptively transition between improving its localization accuracy and exploring the environment to maximize information gain about a spatial field. The controller is designed to guide the robots through three distinct phases: *AP localization*, *field learning*, and *coverage* based on the uncertainties in the estimates and elapsed time.

At each time step t, robot i updates its position $\mathbf{p}_i(t) \in \mathbb{R}^d$ according to the following control law:

$$\dot{p}_i(t) = -\kappa_c \left(\mathbf{p}_i(t) - \mathbf{p}_i^{\text{des}}(t)\right), \quad \kappa > 0, \tag{10}$$

where $\mathbf{p}_i^{\text{des}}(t)$ is the desired position computed as:

$$\begin{aligned} \mathbf{p}_i^{\text{des}}(t) &= (1-\gamma_i(t))\left[(1-\tau_i(t))\mathbf{p}_i^g(t) + \tau_i(t)\mathbf{p}_i^l(t)\right] \\ &+ \gamma_i(t)\mathbf{C}_i(t), \end{aligned} \tag{11}$$

Here, κ_c is a control gain and $\mathbf{p}_i^g(t)$ is the target position for maximizing information gain about the field distribution, $\mathbf{p}_i^l(t)$ is the target position for improving the AP localization accuracy, $\mathbf{C}_i(t)$ is the centroid of robot i's Voronoi cell, and $\tau_i(t), \gamma_i(t) \in [0,1]$ are weighting functions that regulate the robot's focus between these three different objectives.

The target positions are determined by maximizing the information gain within the robot's local domain $\mathcal{D}_i$:

$$\begin{aligned} \mathbf{p}_i^g(t) &= \underset{q \in \mathcal{D}_i}{\text{argmax}}; I^{\text{field}}(q), \\ \mathbf{p}_i^l(t) &= \underset{q \in \mathcal{D}_i}{\text{argmax}}; I^{\text{AP}}(q), \end{aligned} \tag{12}$$

where I_q^{field} and I_q^{AP} are the information gains at point q for the field and AP localization, respectively, computed using the GP-UCB criterion as Eq. (8).

The weighting functions $\tau_i(t)$ and $\gamma_i(t)$ adaptively adjust the robot's behavior based on uncertainty measures and time:

$$\begin{aligned} \tau_i(t) &= S\left(\sigma^{2^{\text{AP}}}(t)\right)(1 - S(t)), \\ \gamma_i(t) &= S\left(\bar{\sigma^2}^{\text{field}}(t)\right)(1 - S(t)), \end{aligned} \tag{13}$$

where $\sigma^{2^{\text{AP}}}(t)$ is the variance of the estimated AP location, $\bar{\sigma^2}^{\text{field}}(t)$ is the average variance of the field distribution over $\mathcal{D}_i$, and $S(\cdot)$ is a sigmoid function defined as:

$$S(x) = \frac{1}{1 + e^{-s(x-\epsilon)}}, \tag{14}$$

with $s > 0$ controlling the steepness of the transition and ϵ being the threshold for variance or time. The inclusion of the time-dependent term $S(t)$ ensures progression through the phases even if variance thresholds are not met. Each robot computes a Voronoi partition of the workspace centered around its current estimate of the AP position $\mathbf{p}^{\text{AP}}(t)$ using AP-oriented partitioning as Eq. (7).

The controller facilitates transitions between different operational phases:

a) Phase 1: AP Localization: When $\sigma^{2^{\text{AP}}}$ is high, $\tau_i(t) \approx 1$, and the robot focuses on improving its localization by moving towards $\mathbf{p}_i^l(t)$. This phase ensures the robot has an accurate frame of reference (FoR).

b) Phase 2: Field Learning: As $\sigma^{2^{\text{AP}}}$ decreases, $\tau_i(t)$ reduces towards 0, shifting focus to maximizing information gain about the field by moving towards $\mathbf{p}_i^g(t)$.

c) Phase 3: Coverage: When the average field variance $\bar{\sigma^2}^{\text{field}}$ decreases, $\gamma_i(t)$ increases, guiding the robot towards the centroid $\mathbf{C}_i(t)$ to enhance coverage.

1) Information Gain Computation: The information gains at a location q for AP localization and field learning are computed using GP-UCB with different α and β values:

$$\begin{aligned} I^{\text{AP}}(q) &= \alpha^{\text{AP}}\mu^{\text{AP}}(q) + \beta^{\text{AP}}\sigma^{2^{\text{AP}}}(q),\ \alpha^{\text{AP}} = 0.5; \beta^{\text{AP}} = 0.5, \\ I^{\text{field}}(q) &= \alpha^{\text{field}}\mu^{\text{field}}(q) + \beta^{\text{field}}\sigma^{2^{\text{field}}}(q),\ \alpha^{\text{field}} = 1; \beta^{\text{field}} = 0, \end{aligned} \tag{15}$$

Setting $\alpha^{\text{AP}} = \beta^{\text{AP}} = 0.5$ balances exploration and exploitation for AP localization, while $\alpha^{\text{field}} = 1.0$ prioritizes areas with higher predicted mean values in field learning.

The proposed controller can be viewed as a weighted combination of gradient ascent steps toward maximizing information gain and coverage optimization. The control input in Eq. (10) can be interpreted as moving towards a weighted centroid of target positions, where the weights are dynamically adjusted based on uncertainty measures.

Assuming that the information gain functions $I^{\text{AP}}(q)$ and $I^{\text{field}}(q)$ are differentiable, the target positions $\mathbf{p}_i^l(t)$ and $\mathbf{p}_i^g(t)$ can be approximated using gradient ascent:

$$\begin{aligned} \mathbf{p}_i^l(t) &\approx \mathbf{p}^i(t) + \eta \nabla I^{\text{AP}}(q)\big|q = \mathbf{p}_i(t), \\ \mathbf{p}_i^g(t) &\approx \mathbf{p}^g(t) + \eta \nabla I^{\text{field}}(q)\big|q = \mathbf{p}_i(t), \end{aligned} \tag{16}$$

where $\eta > 0$ is a step size. Substituting these approximations into Eq. (11) and results to Eq. (10) provides a control law that inherently drives the robot towards regions of high information gain. For more details on the information function variants and their effect, see [33].

E. Parameters Selection

Uncertainty in GPR is essential for informative path planning, where it is commonly used to assess convergence and guide transitions. For example, Mantovani et al. [16] used an uncertainty threshold to determine sample inclusion (filtering noisy samples, which increases uncertainty), while [34] employed variance thresholds to shift from learning the distribution to moving towards mean values. Such thresholds are typically estimated based on the environment size and prior knowledge of the underlying distribution.

The time-dependent term $S(t)$ prevents indefinite stalling in learning phases when variance thresholds may not be achieved due to environmental constraints. Without $S(t)$, the system could remain in localization or learning phases indefinitely if noise levels prevent variance reduction below specified thresholds. This term ensures mission progress while maintaining the uncertainty-driven nature of our approach.

F. Theoretical Analysis

Here, we theoretically analyze the convergence of the proposed control law for AO-IPP and present the main results.

Theorem 1: The proposed control law in Eq. (10) ensures convergence under the following definitions: A *threshold* ϵ_{th} represents the acceptable level of localization uncertainty; a *peak* denotes the maximum achievable information gain given current robot positions and field estimates. As localization variance $\sigma^2_{AP}(t)$ decreases below ϵ_{th}, robot positions $p_i(t)$ converge to desired positions $p_i^{des}(t)$, and information gain approaches its local maximum.

Proof: Define the error between the actual and desired positions as $\mathbf{e}_i(t) = \mathbf{p}_i(t) - \mathbf{p}_i^{\text{des}}(t)$. The error dynamics under the control law can be expressed as:

$$\dot{\mathbf{e}}_i(t) = -\kappa \left(\mathbf{e}_i(t) - \dot{\mathbf{p}}_i^{\text{des}}(t)\right), \kappa > 0, \tag{17}$$

Consider the Lyapunov function [35] $V_i(t) = \frac{1}{2}\|\mathbf{e}_i(t)\|^2$, whose derivative is: $\dot{V}_i(t) = -\kappa\|\mathbf{e}_i(t)\|^2 - \mathbf{e}_i^\top(t)\dot{\mathbf{p}}_i^{\text{des}}(t)$.

We bound the cross term involving $\dot{\mathbf{p}}_i^{\text{des}}(t)$ and show that $\dot{V}_i(t) \leq 0$, leading to a non-increasing Lyapunov function. By Barbalat's Lemma [36], we conclude that $\mathbf{e}_i(t) \to \mathbf{0}$ as $t \to \infty$, which implies that $\mathbf{p}_i(t)$ converges to $\mathbf{p}_i^{\text{des}}(t)$.

As uncertainties decrease and approach a threshold, the desired positions stabilize, leading to maximized information gain. The error dynamics become linear as $\dot{\mathbf{p}}_i^{\text{des}}(t) \to 0$, ensuring exponential convergence. Thus, the control law ensures that the location uncertainty reduces, and information gain increases over time until it peaks. ■

Theorem 2 (Regret Analysis): Let T denote the time horizon over which a multi-robot system operates, with each robot i estimating the position of a common anchor, modeled by a Gaussian distribution $N(\mu_i^{\text{AP}}, \sigma_i^{2\,\text{AP}})$, where μ_i^{AP} is the estimated mean and $\sigma_i^{2\,\text{AP}}$ is the variance of the anchor position estimate for robot i. Define the cumulative regret $R(T)$ as the sum of the difference between the actual outcomes and the best possible outcomes under optimal conditions for each step t, where outcomes refer specifically to localization accuracy and coverage quality, comprising suboptimal actions due to both estimation inaccuracies and coverage positioning errors. We have:

$$R(T) \leq \mathcal{O}\left(\sqrt{T(1 + \bar{\sigma^2}^{\text{AP}}(t)) + \mathcal{L}(T)}\right), \tag{18}$$

where $\bar{\sigma^2}^{\text{AP}}(t)$ is the average variance across all robots in the Gaussian noise affecting the anchor position estimation, and $\mathcal{L}(T)$ represents the cumulative learning cost over T steps.

Proof: The cumulative learning cost $\mathcal{L}(T)$ is defined as:

$$\mathcal{L}(T) = \sum_{t=1}^{T} \int_{\mathcal{D}} \left(\phi(q) - \phi^{(t)}(q)\right)^2 dq, \tag{19}$$

where $\phi^{(t)}(\cdot)$ represents the estimated density function at time t, and $\mathcal{D}$ is the domain for the density function.

The regret function $r(t)$ accounts for errors in anchor position estimation and learning inaccuracies at a time instant t:

$$r(t) = \sum_{i=1}^{n} \mathcal{H}\left(\phi_i(t), \boldsymbol{x}(t)\right) - \min_{\boldsymbol{x}} \mathcal{H}\left(\phi_i, \boldsymbol{x}\right), \tag{20}$$

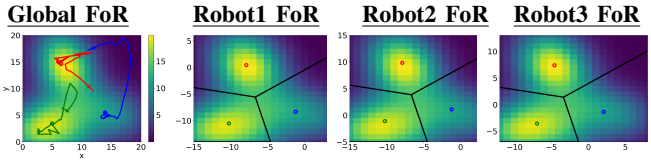

Fig. 2. Scenario 1 results: The left-most figure illustrates the ground truth and the trajectories of robot 1 (red), robot 2 (green), and robot 3 (blue) after completing the localization phase. The remaining figures display the predicted distributions from each robot's frame of reference (FoR).

The cumulative regret $R(T)$ accounts for errors in anchor position estimation and learning inaccuracies. The locational error is bounded by the variance σ_i^2 of the Gaussian estimation model, and the learning error is captured by $\mathcal{L}(T)$. Using standard GP regret bounds, the cumulative regret is upper-bounded by:

$$R(T) \leq O\left(\sqrt{T\left(1 + \bar{\sigma}^{2\text{AP}}\right) + \mathcal{L}(T)}\right), \tag{21}$$

The bound follows from decomposing the regret into localization and learning components. The localization error contributes $O(\sqrt{T\bar{\sigma}^2_{AP}})$ to the cumulative regret, while the learning error contributes $\mathcal{L}(T)$. Using the triangle inequality:

$$\begin{aligned} R(T) &\leq \sqrt{T} \cdot \max(\text{localization error}) + \mathcal{L}(T) \\ &\leq O\left(\sqrt{T(1 + \bar{\sigma}^2_{AP}) + \mathcal{L}(T)}\right), \end{aligned}$$

As $T \to \infty$, both the estimation variance and the learning cost diminish due to improved position estimates and field distribution learning. Consequently:

$$R(T) \to \mathcal{O}\left(\sqrt{T}\right) \quad \text{as} \quad \bar{\sigma^2}^{\text{AP}}, \mathcal{L}(T) \to 0, \tag{22}$$

Thus, the cumulative regret bound reflects the system's improvement over time as both locational error and learning uncertainties reduce. ■

IV. Experiments and Results

We conducted comprehensive evaluations in simulation environments of $20 \times 20\,m^2$ (N=3) and $40 \times 40\,m^2$ (N=6) using the Robotarium platform [37], supplemented by real-world dataset validation and hardware testbed experiments. Performance assessment employed three key metrics: cumulative regret $r(t)$ from Eq. (20), Average Localization Error (ALE) defined as $\text{ALE}_i = ||p_i^{\text{AP}} - p_i^{\text{AP}}(t)||$, and Root Mean Square Error (RMSE) calculated as $\text{RMSE}_i = \sqrt{\frac{1}{\mathcal{D}}\int_{\mathcal{D}}(\phi_i - \phi_i(t))^2}$, where $\phi_i(t)$ and $p_i^{\text{AP}}(t)$ represent predicted spatial density and anchor point position in robot i's frame of reference at time t.

The experimental configuration maintained robot velocity at $1\,m/s$ with iterative target position reevaluation using our control law. Initial anchor point estimation utilized 10 random samples within the communication radius to establish baseline position and uncertainty estimates. The parameter setting $\beta^{\text{field}} = 0$ in Eq. (15) during Phase 2 prioritizes exploitation of areas with higher predicted mean values rather than exploration of high-variance regions, reflecting the transition from exploration-focused sampling to coverage-oriented positioning.

TABLE I: KEY PERFORMANCE METRICS COMPARING THE AO-IPP AND VEC (VORONOI BASED ENVIRONMENTAL COVERAGE) APPROACHES.

Experiment	Convergence Iterations (γ)			Regret $r(t)$			RMSE - Field			Variance - Field $\bar{\sigma}^{2^{\text{field}}}$		
	VEC (GPS)	AO-IPP (GPS)	AO-IPP (No GPS)	VEC (GPS)	AO-IPP (GPS)	AO-IPP (No GPS)	VEC (GPS)	AO-IPP (GPS)	AO-IPP (No GPS)	VEC (GPS)	AO-IPP (GPS)	AO-IPP (No GPS)
Sim Sc. 1	101	41	120	0.13	0.01	0.03	1.3	0.8	1.4	1.1	1.3	1.7
Sim Sc. 2	131	161	161	0.18	0.01	0.05	2.0	0.92	1.4	1.7	2.7	2.4
Dataset Temperature	60	81	60	0.05	0.01	0.09	1.08	0.96	1.12	1.04	1.4	1.3
Dataset Humidity	77	84	80	0.02	0.01	0.01	1.25	0.8	1.3	0.54	0.9	0.8
In-House Robots	63	63	64	0.07	0.01	0.1	0.7	0.35	1.4	0.9	0.9	4.9

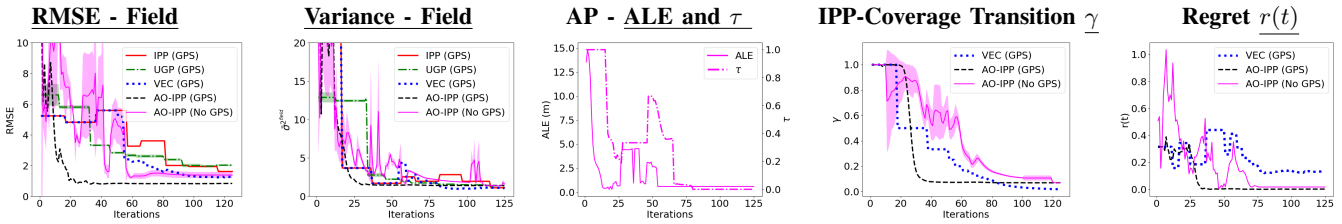

Fig. 3. Performance results of studied controllers with three robots (Scenario 1): The plots show the evolution of RMSE, Variance (uncertainty) of the predicted spatial field with IPP, Average Localization error (ALE), regret metric as well as the parameters τ (indicating the shift from localization to path planning) and γ (indicating the shift from path planning to coverage), depicting both the mean and standard deviation across all robots.

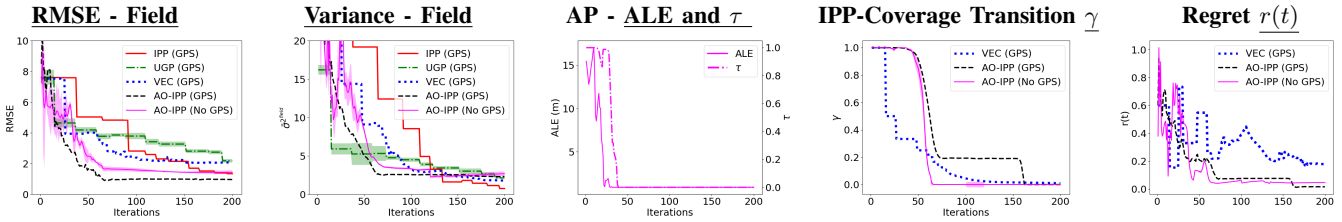

Fig. 4. Performance results of studied controllers with six robots (Scenario 2) with plots similar to Fig. 3).

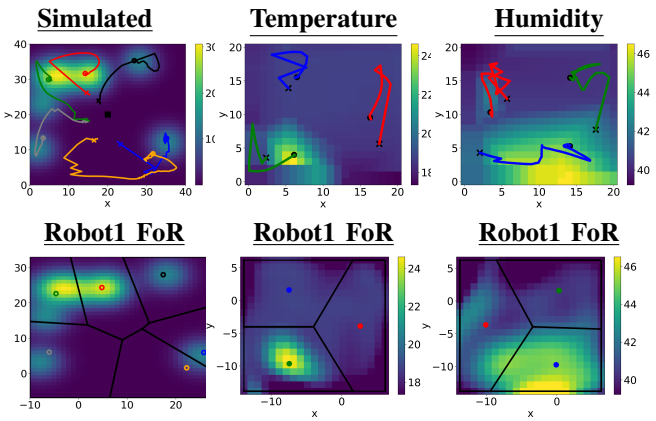

Fig. 5. The ground truth (top) and predicted (bottom) spatial field distributions for Scenario 2 (left) and real datasets—temperature (center) and humidity (right)—are presented along with AO-IPP (No GPS) trajectories after completing the localization phase.

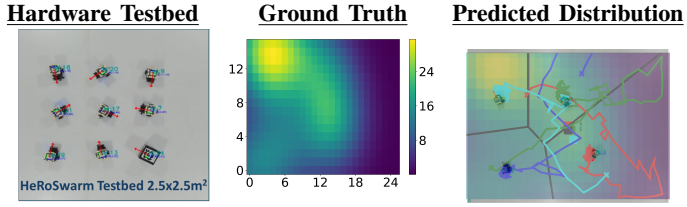

Fig. 6. AO-IPP demonstration on an in-house swarm robotics testbed.

We compare our approach against three established baselines: IPP, a GPS-based distributed method targeting maximum field variance locations [26]; Uncertain GP (UGP), incorporating GPS localization uncertainty modeled as zero-mean Gaussian noise with 1m standard deviation [3]; and VEC, employing time-driven transitions from sampling to coverage using $\gamma = \frac{1}{t}$ [17].

Additionally, we evaluate AO-IPP with GPS to validate uncertainty-driven transitions against fixed time-bounded approaches. For AP and Field distributions, we added zero-mean Gaussian noises with a variance of $4dBm^2$. According to this domain, we set ϵ values in Eq. (14).

A. Simulation Experiments

We ran two simulation scenarios (I and II) with 5 trials, each under two density functions, to demonstrate applicability in various settings. In addition, we evaluate the proposed controller on real-world datasets and in an in-house swarm robotics testbed. A summary of the key results compared to VEC is provided in Table I.

Scenario I (N=3 Robots): The three-robot configuration provided foundational validation of our uncertainty-driven phase transition methodology. Figures 2 and 3 demonstrate the systematic progression through localization, learning, and coverage phases. The proposed AO-IPP controller without GPS initially prioritized positions critical for accurate anchor point prediction, achieving rapid Average Localization Error reduction as evidenced by the ALE trajectory plots. The transition parameter τ clearly illustrates the smooth progression from localization focus to spatial distribution learning as anchor point estimates achieved sufficient accuracy.

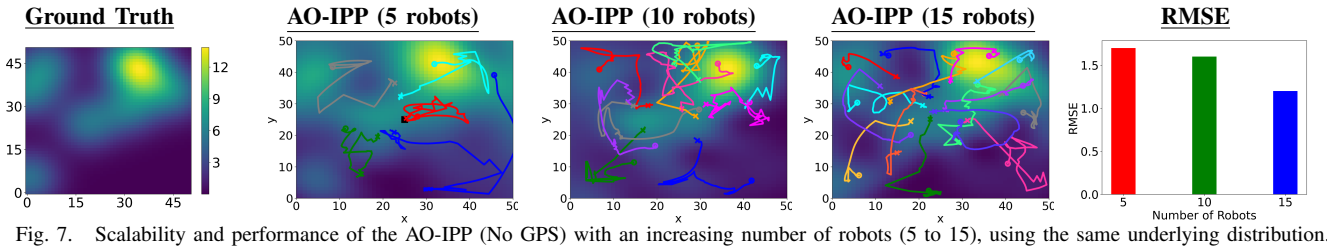

Fig. 7. Scalability and performance of the AO-IPP (No GPS) with an increasing number of robots (5 to 15), using the same underlying distribution.

AO-IPP (No GPS) reduces the RMSE to 1.4, achieving improvements of 14% and 44% over UGP and IPP, respectively, while remaining 7% higher than VEC. This slight lag in distribution reconstruction is attributed to inaccuracies in predicted positions. However, the proposed approach outperforms VEC by approximately 3× in terms of regret. This demonstrates the importance of uncertainty-driven transitions of the path objectives from reducing the uncertainty of localization to IPP to coverage, compared to time-bounded VEC's transitions. On the other hand, when GPS is available, our proposed *AO-IPP (GPS)* variant surpasses VEC in RMSE reduction by approximately 62% while also achieving 13× lower regret value.

Scenario II (N=6 Robots): Fig. 4 shows the results of this scenario, highlighting the approach's effectiveness in larger environments. Similar to Scenario I, the controller successfully transitions from AP estimation to variance reduction of the spatial distribution. AO-IPP (No GPS) achieves outperforms UGP and VEC in RMSE reduction by 36% and 30%, respectively. However, AO-IPP (No GPS) lags behind IPP by 3%. In terms of regret, AO-IPP (No GPS) outperforms VEC (GPS) by 54%. Similar to Scenario 1, AO-IPP (GPS), when global position availability is considered, the proposed approach surpasses all existing approaches in both learning and coverage. Specifically, it achieves a 35% and 54% lower RMSE than IPP and VEC, respectively, and outperforms VEC in regret by a factor of 18×, highlighting the effectiveness of uncertainty-driven transitions from learning to coverage objectives over fixed transitions used in VEC [17] and Mantovani et al [16]. For brevity, only the predicted mean from Robot 1's frame of reference is presented in Fig. 5.

B. Real-world Dataset Experiments

We present the outcomes of the AO-IPP controller applied to real-world datasets from the Intel Berkeley Lab[1]. It consists of sensory data collected from 54 stationary sensors installed in an office ($20 \times 20m^2$), measuring humidity, temperature, light intensity, etc. For our experiment, we focus on utilizing the temperature and humidity data. The results of these experiments are depicted in Table I and Fig. 5. AO-IPP (No GPS) closely matches VEC short by 3% and 4% in terms of RMSE, but it outperforms VEC in terms of regret by a factor of 2 for the temperature data set, while lag behind by a factor of 1.1 for the humidity dataset. The AO-IPP (GPS) variant remedies these minor lags due to initial localization phase efforts, outperforming all other variants, as observed before. These findings emphasize the efficacy of the proposed AO-IPP (No GPS) approach in localizing the AP position, spatial field learning, and coverage, all while relaxing the reliance on GPS availability.

[1]http://db.csail.mit.edu/labdata/labdata.html

C. Real-world In-House Robot Experiments

This section demonstrates the effectiveness of the proposed approach using an in-house swarm robotics testbed. Four robots are deployed on a 2.5×1.5 m^2 testbed, with a robot velocity set at 0.2 m/s. To meet the localization requirements of our approach, we scale the environment by a factor of 10. Figure 6 presents the ground truth and the robot trajectories using the AO-IPP (No GPS). The detailed results are shown in Table. I. The proposed approach achieved a regret value of 0.07, which is 22% higher than the VEC approach and 85.71% higher than its GPS-based variant. While the regret is higher for AO-IPP (No GPS) than VEC in this scenario, this can be attributed to localization noise. A comparison with AO-IPP (GPS) demonstrates that the proposed transition function offers a significant advantage over the VEC approach. These results corroborate the simulations, confirming the effectiveness of AO-IPP in balancing learning and coverage objectives.

Scalability Analysis: Systematic evaluation with 5 to 15 robots demonstrated 25% RMSE improvement with increased robot count. Enhanced data sample availability and inter-robot localization efficiency confirmed the framework's scalability for larger deployments. The results for this scenario are presented in Fig. 7.

Model Behavior: The dual-GP architecture enables specialized uncertainty source handling but introduces coordination challenges during phase transitions, explaining observed RMSE variance. Regret fluctuations reflect natural exploration-exploitation tensions during uncertainty-driven transitions, validating theoretical predictions regarding multi-objective balancing challenges.

V. Conclusion

This work addressed the fundamental challenge of multi-robot IPP in GPS-denied environments by the introduction of the AO-IPP framework that enables coordinated multi-robot teams to simultaneously localize using relative anchor point measurements, learn spatial field distributions, and achieve coverage optimization without global reference frames. Comprehensive experimental validation across simulations, real-world datasets, and hardware testbeds demonstrated that AO-IPP achieves performance comparable to GPS-based algo-

rithms while operating entirely without global positioning, outperforming fixed time-based methods with up to 54% improvement in balancing objectives. The framework exhibited sublinear regret bounds and robust scalability across varying team sizes. When GPS availability was assumed, AO-IPP demonstrated superior performance, validating that uncertainty-based transitions provide fundamental advantages over temporal scheduling approaches. While the dual-GP architecture introduces coordination challenges during transitions, the framework successfully enables autonomous coordination in challenging environments previously inaccessible to traditional methods.

REFERENCES

[1] K.-C. Ma, Z. Ma, L. Liu, and G. S. Sukhatme, "Multi-robot informative and adaptive planning for persistent environmental monitoring," in *Distributed Autonomous Robotic Systems: The 13th International Symposium*. Springer, 2018, pp. 285–298.

[2] S. Bai, T. Shan, F. Chen, L. Liu, and B. Englot, "Information-driven path planning," *Current Robotics Reports*, vol. 2, no. 2, 2021.

[3] M. Popović, T. Vidal-Calleja, J. J. Chung, J. Nieto, and R. Siegwart, "Informative path planning for active field mapping under localization uncertainty," in *2020 IEEE International Conference on Robotics and Automation (ICRA)*, 2020, pp. 10 751–10 757.

[4] S. Manjanna, A. Q. Li, R. N. Smith, I. Rekleitis, and G. Dudek, "Heterogeneous multi-robot system for exploration and strategic water sampling," in *2018 IEEE international conference on robotics and automation (ICRA)*. IEEE, 2018, pp. 4873–4880.

[5] A. Carron, M. Todescato, R. Carli, L. Schenato, and G. Pillonetto, "Multi-agents adaptive estimation and coverage control using gaussian regression," in *2015 European Control Conference (ECC)*. IEEE, 2015, pp. 2490–2495.

[6] A. Viseras, D. Shutin, and L. Merino, "Online information gathering using sampling-based planners and gps: An information theoretic approach," in *2017 IEEE/RSJ International Conference on Intelligent Robots and Systems (IROS)*. IEEE, 2017, pp. 123–130.

[7] B. Woosley, P. Dasgupta, J. G. Rogers III, and J. Twigg, "Multi-robot information driven path planning under communication constraints," *Autonomous Robots*, vol. 44, no. 5, pp. 721–737, 2020.

[8] G. A. Di Caro and A. W. Z. Yousaf, "Multi-robot informative path planning using a leader-follower architecture," in *2021 IEEE International Conference on Robotics and Automation (ICRA)*. IEEE, 2021, pp. 10 045–10 051.

[9] R. Wehbe and R. K. Williams, "Probabilistically resilient multi-robot informative path planning," *arXiv preprint arXiv:2206.11789*, 2022.

[10] S. Kemna, J. G. Rogers, C. Nieto-Granda, S. Young, and G. S. Sukhatme, "Multi-robot coordination through dynamic voronoi partitioning for informative adaptive sampling in communication-constrained environments," in *2017 IEEE International Conference on Robotics and Automation (ICRA)*. IEEE, 2017, pp. 2124–2130.

[11] A. Singh, A. Krause, C. Guestrin, and W. J. Kaiser, "Efficient informative sensing using multiple robots," *Journal of Artificial Intelligence Research*, vol. 34, pp. 707–755, 2009.

[12] J. A. Placed, J. Strader, H. Carrillo, N. Atanasov, V. Indelman, L. Carlone, and J. A. Castellanos, "A survey on active simultaneous localization and mapping: State of the art and new frontiers," *IEEE Transactions on Robotics*, vol. 39, no. 3, pp. 1686–1705, 2023.

[13] F. Chen, J. D. Martin, Y. Huang, J. Wang, and B. Englot, "Autonomous exploration under uncertainty via deep reinforcement learning on graphs," in *2020 IEEE/RSJ International Conference on Intelligent Robots and Systems (IROS)*. IEEE, 2020, pp. 6140–6147.

[14] M. Tzes, N. Bousias, E. Chatzipantazis, and G. J. Pappas, "Graph neural networks for multi-robot active information acquisition," *arXiv preprint arXiv:2209.12091*, 2022.

[15] L. Schmid, M. Pantic, R. Khanna, L. Ott, R. Siegwart, and J. Nieto, "An efficient sampling-based method for online informative path planning in unknown environments," *IEEE Robotics and Automation Letters*, vol. 5, no. 2, pp. 1500–1507, 2020.

[16] M. Mantovani, F. Pratissoli, and L. Sabattini, "Distributed coverage control for spatial processes estimation with noisy observations," *IEEE Robotics and Automation Letters*, vol. 9, no. 5, pp. 4431–4438, 2024.

[17] M. Santos, U. Madhushani, A. Benevento, and N. E. Leonard, "Multi-robot learning and coverage of unknown spatial fields," in *2021 International Symposium on Multi-Robot and Multi-Agent Systems (MRS)*. IEEE, 2021, pp. 137–145.

[18] Y.-H. Kim, D. A. Shell, C. Ho, and S. Saripalli, "Spatial interpolation for robotic sampling: Uncertainty with two models of variance," in *Experimental Robotics: The 13th International Symposium on Experimental Robotics*. Springer, 2013, pp. 759–774.

[19] K. Jakkala and S. Akella, "Multi-robot informative path planning from regression with sparse gaussian processes," *arXiv preprint arXiv:2309.07050*, 2023.

[20] Y. Min, S. S. Park, and H.-L. Choi, "Informative planning of mobile sensor networks in gps-denied environments," in *AIAA Scitech 2020 Forum*, 2020, p. 1342.

[21] D. Jang, J. Yoo, C. Y. Son, and H. J. Kim, "Fully distributed informative planning for environmental learning with multi-robot systems," *arXiv preprint arXiv:2112.14433*, 2021.

[22] Y. Brouwer, A. Vale, and R. Ventura, "Informative path planner with exploration–exploitation trade-off for radiological surveys in non-convex scenarios," *Robotics and Autonomous Systems*, vol. 136, p. 103691, 2021.

[23] T. Yang, Y. Cao, and G. Sartoretti, "Intent-based deep reinforcement learning for multi-agent informative path planning," in *2023 International Symposium on Multi-Robot and Multi-Agent Systems (MRS)*. IEEE, 2023, pp. 71–77.

[24] Y. Shi, N. Wang, J. Zheng, Y. Zhang, S. Yi, W. Luo, and K. Sycara, "Adaptive informative sampling with environment partitioning for heterogeneous multi-robot systems," in *2020 IEEE/RSJ international conference on intelligent robots and systems (IROS)*. IEEE, 2020, pp. 11 718–11 723.

[25] W. Luo, C. Nam, G. Kantor, and K. Sycara, "Distributed environmental modeling and adaptive sampling for multi-robot sensor coverage," in *Proceedings of the 18th International Conference on Autonomous Agents and MultiAgent Systems*, 2019, pp. 1488–1496.

[26] A. Benevento, M. Santos, G. Notarstefano, K. Paynabar, M. Bloch, and M. Egerstedt, "Multi-robot coordination for estimation and coverage of unknown spatial fields," in *2020 IEEE international conference on robotics and automation (ICRA)*. IEEE, 2020, pp. 7740–7746.

[27] A. A. R. Newaz, M. Alsayegh, T. Alam, and L. Bobadilla, "Decentralized multi-robot information gathering from unknown spatial fields," *IEEE Robotics and Automation Letters*, vol. 8, no. 5, 2023.

[28] A. Munir, E. Latif, and R. Parasuraman, "Anchor-oriented localized voronoi partitioning for gps-denied multi-robot coverage," in *2024 IEEE/RSJ International Conference on Intelligent Robots and Systems (IROS)*. IEEE, 2024, pp. 3395–3402.

[29] J. Cortes, S. Martinez, T. Karatas, and F. Bullo, "Coverage control for mobile sensing networks," *IEEE Transactions on robotics and Automation*, vol. 20, no. 2, pp. 243–255, 2004.

[30] S. Lloyd, "Least squares quantization in pcm," *IEEE transactions on information theory*, vol. 28, no. 2, pp. 129–137, 1982.

[31] W. Gosrich, S. Mayya, R. Li, J. Paulos, M. Yim, A. Ribeiro, and V. Kumar, "Coverage control in multi-robot systems via graph neural networks," in *2022 International Conference on Robotics and Automation (ICRA)*. IEEE, 2022, pp. 8787–8793.

[32] W. Luo and K. Sycara, "Adaptive sampling and online learning in multi-robot sensor coverage with mixture of gaussian processes," in *2018 IEEE international conference on robotics and automation (ICRA)*. IEEE, 2018, pp. 6359–6364.

[33] A. Munir and R. Parasuraman, "Exploration–exploitation tradeoff in the adaptive information sampling of unknown spatial fields with mobile robots," *Sensors*, vol. 23, no. 23, p. 9600, 2023.

[34] D. Jang, J. Yoo, C. Y. Son, D. Kim, and H. J. Kim, "Multi-robot active sensing and environmental model learning with distributed gaussian process," *IEEE Robotics and Automation Letters*, vol. 5, no. 4, pp. 5905–5912, 2020.

[35] V. Lakshmikantham, V. M. Matrosov, and S. Sivasundaram, *Vector Lyapunov functions and stability analysis of nonlinear systems*. Springer Science & Business Media, 2013, vol. 63.

[36] Z. Wu, Y. Xia, and X. Xie, "Stochastic barbalat's lemma and its applications," *IEEE Transactions on Automatic Control*, vol. 57, no. 6, pp. 1537–1543, 2011.

[37] S. Wilson, P. Glotfelter, S. Mayya, G. Notomista, Y. Emam, X. Cai, and M. Egerstedt, "The robotarium: Automation of a remotely accessible, multi-robot testbed," *IEEE Robotics and Automation Letters*, vol. 6, no. 2, pp. 2922–2929, 2021.